Temperature Scaling Method for Markov Chains

Lonnie D. Crosby and Theresa L. Windus*

Department of Chemistry, Iowa State University and Ames Laboratory, Ames, Iowa 50010

Received: June 27, 2008; Revised Manuscript Received: October 27, 2008

The use of ab initio potentials in Monte Carlo simulations aimed at investigating the nucleation kinetics of water clusters is complicated by the computational expense of the potential energy determinations. Furthermore, the common desire to investigate the temperature dependence of kinetic properties leads to an urgent need to reduce the expense of performing simulations at many different temperatures. A method is detailed that allows a Markov chain (obtained via Monte Carlo) at one temperature to be scaled to other temperatures of interest without the need to perform additional large simulations. This Markov chain temperature-scaling (TeS) can be generally applied to simulations geared for numerous applications. This paper shows the quality of results which can be obtained by TeS and the possible quantities which may be extracted from scaled Markov chains. Results are obtained for a 1-D analytical potential for which the exact solutions are known. Also, this method is applied to water clusters consisting of between 2 and 5 monomers, using Dynamical Nucleation Theory to determine the evaporation rate constant for monomer loss. Although ab initio potentials are not utilized in this paper, the benefit of this method is made apparent by using the Dang−Chang polarizable classical potential for water to obtain statistical properties at various temperatures.

1. Introduction

The temperature dependence of thermally accessible regions of the potential energy surface generally requires that Monte Carlo[1,2] (MC) simulations be performed separately for each temperature of interest. This situation leads to the execution of many simulations, each differing only by temperature. These additional simulations, although computationally demanding, do not usually suffer from a bottleneck condition in computational resources due to the availability of fast classical potentials, such as the Effective Fragment Potential,[3] TIP4P,[4] and Dang−Chang[5] potentials for water. However, with the development of petascale supercomputing platforms and more efficient parallel algorithms, it is conceivable that more expensive ab initio methodologies[6] could be utilized in these MC simulations. With the additional computational expense that ab initio electronic structure calculations would impose, it becomes very important to reuse the data from every simulation as much as possible. While it is possible to perform one ab initio simulation on small systems at a particular temperature, it becomes prohibitively expensive to perform 5 or 10 simulations at different temperatures. In this paper, a temperature-scaling method (TeS) is developed in an attempt to "reuse" the results of a MC simulation at one temperature (T_1) and produce results (with relatively little computational overhead) at another temperature (T_2) or a set of temperatures. This method is applied to a 1-D model potential and to water cluster simulations.

2. Temperature-Scaling (TeS)

As mentioned above, Markov Chain Monte Carlo[1,2] (MCMC) methods are performed separately at each temperature of interest. The rational lies in the fact that temperature is a parameter that affects the composition of the resulting Markov chain. As a result the statistical properties obtained from this chain depend on temperature. The computational expense in this approach grows roughly linearly with the number of temperatures desired, the exception being the increase in computational expense due to configurational space becoming more or less thermally accessible. The goal of this research is to increase the number of temperatures for which a single MCMC simulation can provide statistical information.

In the canonical ensemble, the acceptance probability between two states, i and j, within a volume, V, is $P_{ij}(T, V) = \min[1, \exp(-\Delta_{ij}U/k_bT)]$, where the difference in these states' potential energy is $\Delta_{ij}U$, k_b is Boltzmann's constant, and T is the temperature. The use of this acceptance probability to build a Markovian chain of states allows the determination of the state distribution. This distribution of states approaches, as the Markov chain grows, a stationary state distribution which is equivalent to that of the canonical ensemble. The stationary distribution is a Boltzmann weighted distribution of states such that the probability of the occurrence of state i within a volume V in the Markov chain is equal to

$$P_i(T, V) = \frac{g_i \exp\left[-\frac{U_i}{k_bT}\right]}{Q(T, V)} = \frac{N_i(T, V)}{N_{\text{total}}(V)} \tag{1}$$

where U_i is the potential energy of state i, $Q(T, V)$ is the canonical partition function which serves as a normalization constant, and g_i is the degeneracy of state i. This probability is physically encoded within the Markov chain and is obtainable by "counting" the occurrence of states, where $N_i(T, V)$ is the temperature-dependent frequency of state i within a volume V in the Markov chain and $N_{\text{total}}(V)$ is the total number of members in the Markov chain. The Markov chain is, therefore, a truly temperature-dependent entity.

As a result of the ability to "count" the occurrence of states within the Markov chain, each member of the chain has an equal weight of one. Can a different choice of weight, $w_i(T_1, T_2)$, for each state allow a Markov chain obtained at a temperature T_1 to reproduce the stationary distribution at another temperature (T_2)? For example

* Corresponding author. E-mail: theresa@fi.ameslab.gov

10.1021/jp805688j CCC: $40.75
Published on Web 12/24/2008

$$\frac{w_i(T_1, T_2)P_i(T_1, V)}{\sum_i w_i(T_1, T_2)P_i(T_1, V)} = P_i(T_2, V) \quad (2)$$

where $w_i(T_1, T_2)$ denotes the weight of each state i in the Markov chain. By substituting eq 1 into this expression for both $P_i(T_1, V)$ and $P_i(T_2, V)$, it is sufficient to require that the weight be equal to the following.

$$w_i(T_1, T_2) = \exp\left[-\frac{U_i}{k_b}\left(\frac{1}{T_2} - \frac{1}{T_1}\right)\right] \quad (3)$$

The weight for each state i is a constant that only depends on the state's potential energy, U_i, and the temperature change $(1/T_2 - 1/T_1)$, allowing the weights to be determined concurrently with the Markov chain at T_1. These TeS weights act as coefficients to scale the probability of a state at T_1 to the corresponding probability at T_2. With this change in state probability the distribution must be carefully renormalized to preserve the relationship between the canonical partition functions. Considering this renormalization, the partition functions are related by $(\sum_i w_i(T_1, T_2)P_i(T_1, V))Q(T_1, V) = Q(T_2, V)$, which gives a complete transformation of the Markov chain between the temperatures T_1 and T_2.

The structure of the original Markov chain at T_1 is preserved if no scaling is performed ($T_1 = T_2$) giving $w_i(T_1, T_2) = 1$ for every configuration in the chain. If TeS is performed, however, states will change importance in the Markov chain based on their relative potential energy and the temperature change. States will become more important as temperature increases if they possess higher potential energies. These states will, however, become less important as temperature decreases. This behavior mirrors the respective increase and decrease of thermally accessible states as temperature changes.

The TeS method, which is performed with respect to a Markov chain, is very similar to Weighted Histogram analysis.[7] Ferrenberg and Swendson formulated this method to study phase transitions. The goal was to use the results of a single MC simulation performed close to the critical temperature to examine the behavior of systems at temperatures around the critical temperature. The necessity of this approach was to reduce the computational expense and increase the accuracy of critical temperature determinations associated with performing multiple MC simulations at different and discrete temperatures. By using Weighted Histogram analysis, the temperature could be scanned at arbitrary precision, without the need for additional MC simulations, to more accurately determine the critical temperature.

Weighted Histogram analysis[7] is a general method in which a histogram (probability distribution) obtained at one set of conditions (parameters) is scaled to another set of conditions. The probability distribution chosen for Weighted Histogram analysis has the general form in one parameter

$$P_B(A) = \frac{g(B)\exp[-AB]}{Q(B)} \quad (4)$$

where A and B refer to a property and parameter respectively which are necessarily thermodynamic conjugate variables. This is similar to our TeS method where temperature is the varied parameter, except that the quantity being scaled is the probability distribution and not a Markov chain. In our TeS example A is equal to the potential energy, U, and B is equal to $(k_bT)^{-1}$. $Q(B)$ is the canonical partition function, which is defined as a sum over all potential energies, U. The scaling of this potential energy distribution in Weighted Histogram analysis is performed by defining weights to each value of the potential energy similar to eq 3. The result of this formulation is that temperature-scaling can only be performed on histograms of properties for which temperature is the conjugate variable.

The major difference between the Weighted Histogram analysis[7] method and our Markov chain TeS method is the quantity that is scaled. In both methods a MC simulation is performed at a temperature T_1. In Weighted Histogram analysis, this simulation is used to produce a probability distribution at T_1, which is scaled to a new temperature T_2. Alternatively in our TeS method, the underlying Markov chain at T_1 is scaled to a new temperature T_2 that is used to produce the new probability distributions. The advantage of scaling the underlying Markov chain is that probability distributions of properties not conjugate to temperature can be obtained in the same manner as the original Markov chain. TeS is therefore not restricted to probability distributions of the potential energy or other energy derived quantities such as the heat capacity.

Although TeS may be performed with respect to any temperature change, care must be taken to ensure that the scaled Markov chain produces a distribution that is sufficiently close to the stationary probability distribution. Given that the initial Markov chain, at temperature T_1, is sufficiently close to the stationary probability distribution, then the probability that state i occurs within a volume in the chain is given by eq 1. Since no states are added to or deleted from the Markov chain during TeS, the states sampled at T_1, albeit with altered importance, must be able to provide a Markov chain at T_2 that similarly conforms to eq 1. The only way this is rigorously true is if all important states at T_2 are thermally accessible at T_1. Therefore $T_1 \geq T_2$ is a necessary condition. However, at sufficiently high temperatures there is a possibility that not all thermally accessible states are adequately sampled. As temperature increases more states become thermally accessible allowing entropic effects to become increasingly important. This effect enters into the sampling probability, eq 1, through the state degeneracy term.

Ferrenberg and Swendsen[8] give a method that allows the approximation of the maximum temperature change allowed in Weighted Histogram analysis before enthalpic or entropic contributions seriously degrade the quality of the scaled distributions. This approximation is performed on the original distribution (before scaling) and involves estimating the change in temperature that would theoretically produce a certain change in the average potential energy of the system. The heat capacity at constant volume, $C_v = (\partial U/\partial T)_V$, gives this relationship for the canonical ensemble. Assuming that the heat capacity is constant over a temperature range, the temperature change is given by $\Delta T = (\partial T/\partial U)_V \Delta U$. The determination of the maximum temperature change is driven by knowledge of the maximum allowable potential energy change, ΔU. Similar to the arguments above, the average potential energy of the system should not change such that it lies outside of the range of potential energies sampled. Therefore, Ferrenberg and Swendsen use a measure based on the potential energy distribution, the standard deviation of the potential energy ($\sigma(U)$) for the maximum potential energy change. By using this choice for ΔU and the definition of the heat capacity at constant volume for the canonical ensemble, $C_v = \sigma^2(U)/k_bT^2$, the maximum allowed temperature change has an absolute value given in eq 5

$$\Delta T(T_1) = \frac{k_bT_1^2}{\sigma(U)} \quad (5)$$

where T_1 is the temperature of the initial MC simulation. The change in potential energy can be easily changed to any multiple of the standard deviation by multiplication of the right side of eq 5 by the factor.

The goal of this paper is to show the merits and limitations of the TeS method. This goal is accomplished by examining the results of MCMC simulations on some systems of interest. First a 1-D, single-particle analytical potential energy surface is examined with the advantage that the exact probability distributions are available. Second, water clusters of various sizes are examined. Since an exact probability distribution is not known for these systems (as is the case in general) the results of the TeS method are compared to conventional simulations done at each temperature of interest.

3. Comparison between Methodologies

The TeS method is also similar to various Monte Carlo methodologies such as J-Walking,[9] S-Walking,[10] Parallel Tempering[11] (also known as Replica Exchange),[12] and C-Walking.[13] These methodologies try to overcome quasiergodic behavior in low-temperature simulations by sampling from a high-temperature ergodic distribution. J-Walking, S-Walking, Parallel Tempering, and C-walking generally utilize high-temperature distributions which are obtained from concurrent MC simulations. These methods differ from TeS in that they require these additional concurrent MC simulations to obtain a selection of configurations to incorporate in the low-temperature simulation. These methods are also instituted as a sampling methodology in the MC simulation, whereas TeS in performed as a postprocessing step on a completed Markov Chain. J-Walking, S-Walking, Parallel Tempering, and C-Walking differ from one another by the method they use to gain configurations from the high-temperature MC simulation.

J-Walking[9] incorporates configurations into a low-temperature MC simulation from a high-temperature MC simulation based on a probability that may or may not be derived from Metropolis criteria. These high-temperature configurations can be quite different in both configurational space and potential energy than the low-temperature configurations. The difference in configurational space is beneficial in obtaining a more ergodic distribution at low temperature. However, a large difference in potential energy requires additional MC steps to properly thermalize this state to the lower temperature distribution.

S-Walking[10] improves upon this situation by quenching the high-temperature configurations via a steepest decent paradigm such that the potential energy of this state is closer to the potential energy distribution of the low-temperature MC simulation. However, this methodology results in sampling from these quenched configurations which comprise a non-Boltzmann distribution.

Instead of incorporating a high-temperature configuration into a low-temperature MC simulation, Parallel Tempering[11] swaps configurations between the low- and high-temperature MC simulations. This methodology corrects two issues with J-Walking and S-Walking. The potential energy difference between configurations is included in the swapping probability, which ensures that configuration swaps are not allowed between states that differ greatly in potential energy. Also, this swapping probability is based on Metropolis criteria, which takes into account the temperature difference between MC simulations. However, in order to have an acceptable swapping probability the temperature difference between MC simulations must be closely monitored.

C-Walking[13] incorporates the best features of S-Walking and Parallel Tempering methodologies by utilizing high-temperature configuration quenching based on simulated annealing and configuration swapping. This methodology eliminates the need to closely monitor the temperature difference between MC simulations and allows the configuration quenching to be statistically relevant.

Parallel Tempering is sensitive to the temperature difference between MC simulations. For this method to adequately obtain ergodic low-temperature distributions a number of high-temperature MC simulations are required to reach a sufficiently high temperature. The highest temperature should produce an ergodic distribution. The temperature difference between these multiple MC simulations is closely monitored to provide a sufficient swapping probability during the MC simulation. The probability of swapping configurations is given by $\exp[\{-(U_1 - U_2)/k_b\}(1/T_2 - 1/T_1)]$, where $T_1 > T_2$ and U_1refers to the potential energy of a configuration that resides in the high-temperature distribution before swapping. This probability is equal to the product of two TeS weights, $w_1(T_1, T_2)w_2(T_2, T_1$. It is not surprising given this similarity that TeS also suffers from a sensitivity in the temperature difference $|T_2 - T_1|$. This sensitivity is given by eq 5.

The TeS method, unlike J-Walking, S-Walking, C-Walking, and Parallel Tempering, does not require concurrent MC simulations in which to gain configurations. The only requirement is a Markov Chain obtained at a particular temperature. For this method to be used to compensate for quasiergodic behavior at low temperatures, a sufficiently high-temperature MC simulation must be performed. This high-temperature MC simulation must not suffer from quasiergodicity and must be able to be scaled, via TeS, to the low temperature of interest.

4. Analytical Potential

The analytical potential used in this work is a single particle, 1-D potential used previously by Brown and Head-Gordon[13] to compare sampling methodologies. Brown and Head-Gordon defined this as

$$V(x) = \sum_{n=1}^{20} C_n \sin\left(\frac{2n\pi x}{L}\right) \tag{6}$$

where the coefficients $\{C_n\}$ are chosen to be between -1 and 1 and are given in their work. The units of the analytical potential are arbitrary and L refers to the maximum length of the 1-D $\{x\}$ coordinate, which is chosen to be 10.

Figure 1 shows the form of the analytical potential and two exact distribution functions at $T^* = 0.1$ and 3.0. T^* refers to the reduced temperature, which is equal to k_bT, where k_b is Boltzmann's constant and has arbitrary units of energy. However, if units of kcal/mol are assigned to the analytical potential energy and T^*, then $T^* = 3.0$ kcal/mol corresponds to a temperature of $T = 1500$ K and $T^* = 0.1$ kcal/mol corresponds similarly to a temperature of $T = 50$ K. This temperature change is clearly not trivial and produces large changes in the related probability distributions. Furthermore, the potential energy surface is very rough with maximum barrier heights of about 8 kcal/mol and multiple (about 13) recognizable minima. Application of the TeS method on this 1-D analytical potential energy surface is a rigorous and extreme test of this method's ability to completely sample configurational space and produce statistics at two very different temperatures.

This 1-D analytical potential was originally utilized by Brown and Head-Gordon[13] to study solutions to surfaces that demonstrate quasiergodic behavior. Quasiergodicity is a condition in which the Markov chain fails to sample all of the important regions of configurational space. This situation mainly arises due to the inability of a Metropolis Monte Carlo method to transverse regions of low probability which connect regions of

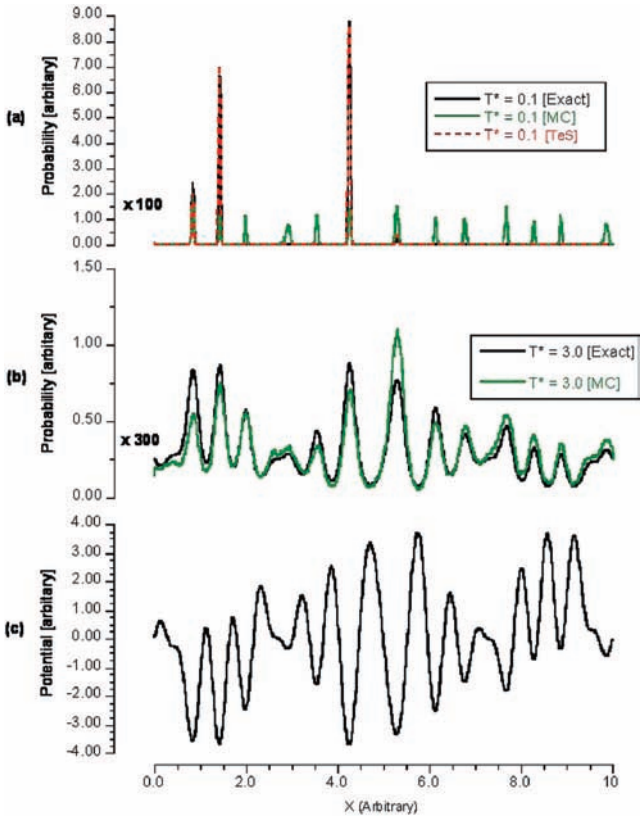

Figure 1. The exact, Monte Carlo (MC) sampled, and TeS probability distributions at (a) $T^* = 0.1$ and (b) $T^* = 3.0$ for a (c) 1-D analytical potential. Of the three distributions in part a, the pair corresponding to the exact and scaled distributions overlap very heavily making them hard to discern from each other. The probability distributions have been scaled by 100 (a) and 300 (b) to better show differences. A total of 100 Markov chains and 4×10^7 configurations are used in the MC simulation.

higher probability. These lower probability regions generally correspond to barriers on the potential energy surface which can confine MC simulations to a subset of available configurational space.

MC simulations are performed on this 1-D analytical potential energy surface at $T^* = 3.0$ and 0.1. Trial moves are attempted with a probability of $^1/_2$ in which the maximum displacement along the coordinate is 0.01. An array of 1000 equally sized bins of width 0.01 are utilized to collect statistical information. The resulting probability distributions are obtained from the average of 100 independent Markov chains. Each Markov chain consists of 4×10^5 configurations for a total of 4×10^7 configurations and have initial configurations evenly distributed along the 1-D coordinate.

Figure 1a shows the probability distribution obtained from a MC simulation at $T^* = 0.1$. At this temperature, $T = 50$ K if the units on the potential are in kcal/mol, every barrier in this rough potential can potentially cause quasiergodicity. The quasiergodicity can be seen in the probability distribution obtained via conventional Metropolis Monte Carlo after 4×10^7 configurations. There are 13 peaks in this probability distribution, one peak for every potential energy well. Each of the 100 Markov chains utilized in this MC calculation remained in the nearest well throughout the entire calculation. Since the Markov chains were unable to surmount the barriers in the potential energy, a series of quasiergodic distributions were produced which do not resemble the exact ergodic distribution also shown in Figure 1a. In contrast, if the entire configurational space was efficiently sampled by these Markov chains the resulting probability distribution would look similar to the exact ergodic distribution. The exact probability distribution has only four regions of probability corresponding to the four lowest potential energy wells. This mismatch between the exact and MC obtained probability distribution demonstrates the problem with quasiergodic Markov chains.

TABLE 1: Percent Peak Area at $T^* = 0.1$ for the Analytical Potential

peak	exact	TeS
1	14.01	12.19
2	34.44	36.75
3	50.11	49.52
4	1.43	2.47

At a much higher temperature ($T^* = 3.0$), the quasiergodicity apparent in the Markov chains is diminished. The probability distribution is shown in Figure 1b for this case. The barriers present in the potential energy do not cause noticeable quasiergodic behavior at this elevated temperature, $T = 1500$ K if the potential energy has units of kcal/mol. Note that the scale in this figure differs by a factor of 3 in order to more clearly show the difference. Because the potential energy barriers have a maximum height of about 8 kcal/mol, the Markov chains have enough energy to explore configurational space fully. Conventional MC simulations at this temperature produce a probability distribution that is very close to the exact ergodic distribution. The sum of the absolute error across the entire distribution reported as a percentage of the sum of the total probability for both distributions is 9.41%. These probability distributions are very spread out across the 1-D coordinate with most minima having some probability, in contrast to the localized nature of the distributions at $T^* = 0.1$.

The TeS method is applied to the Markov chains sampled at $T^* = 3.0$, where each of the 4×10^7 configurations in these Markov chains is given a weight based on eq 3 to produce a corresponding distribution at $T^* = 0.1$. TeS should work well for two related reasons. First, the Markov chains at $T^* = 3.0$ produce a distribution that is sufficiently close to the exact (stationary) distribution, meaning that eq 1 is approximately satisfied. Second, the temperature is sufficiently large enough to overcome the quasiergodicity present at $T^* = 0.1$. Another measure of the feasibility of TeS can be found in the approximate maximum temperature change shown in eq 5. This measure gives information related to the distribution being scaled such as the temperature change that will change the average potential energy of the system to a value that lies outside of the range that is sampled. Performing TeS beyond this limit will adversely affect the quality of results due to the reliance on states which are not adequately sampled. The maximum temperature change determined from the distribution at $T^* = 3.0$ is 2713 K. This range is sufficiently large as to allow the about 1450 K temperature change performed in this work without loss of quality. Figure 1a shows the resulting TeS distribution at $T^* = 0.1$. Like the exact distribution, there are only four regions of probability present. The TeS probability distribution is very close to the exact ergodic distribution. The sum of the absolute error across the entire distribution reported as a percentage of the sum of the total probability for both distributions is 3.73%. To further illustrate the similarity between these distributions, we present in Table 1 the integrated peak heights for the exact and TeS distributions expressed as a percentage of the total. The largest absolute difference is 2.31% between these distributions.

The results above show the utility of the TeS method in two ways. First, the effectiveness of using Markov chain scaling to acquire statistical information at other temperatures is demonstrated. Second, if the original Markov chain is obtained at a temperature that overcomes quasiergodicity concerns then TeS can be utilized to obtain lower temperature distributions free from quasiergodic behavior. However, the 1-D nature of this analytical potential neglects the effects of multidimensional configurational space which include entropic contributions.

5. Water Molecular Clusters

An examination of the effect a multidimensional configurational space has on the TeS method is presented by our work on molecular clusters of water. This examination is done within the context of Dynamical Nucleation Theory (DNT). DNT has been successfully applied previously to water clusters consisting of 2 to 10 monomers.[14] The basis of DNT, discussed elsewhere,[15,16] is to determine the thermodynamic and kinetic properties of nucleation events. This procedure is done via a MC simulation in which a collection of interacting water monomers are described in a spherical volume (defined by its radius). The elementary evaporation process is defined as the loss of a single monomer producing a cluster of size $i - 1$, where i is the number of monomers in the simulation. Expressed as a reaction equation, $N_i \rightarrow N_{i-1} + N_1$, where N denotes concentrations of the various sized molecular clusters, a spherical dividing surface (defined by a radius) serves to define configurations belonging to the i-cluster and those belonging to the $(i - 1)$-cluster plus monomer. The radius (r_{cut}) which defines the molecular cluster of water monomers at a particular temperature is determined by the location of a kinetic bottleneck during this isothermal expansion process. The evaporation rate constant ($\alpha_i(T, r_{cut})$) is proportional to the rate of change in the molecular cluster's Helmholtz free energy with respect to volume. Therefore, the radial probability distribution of water monomers, which is related to the free energy, plays a large role in the determination of the defining radius (r_{cut}) and the evaporation rate constant ($\alpha_i(T, r_{cut})$).[15,16]

Since the exact radial distributions of conformations are not known for these systems, the resulting probability distributions from the TeS method are compared to MC simulations performed at each temperature of interest. The properties obtained from the TeS Markov chain are compared to those obtained from a Markov chain built at the temperature of interest. Application of TeS on this chemical system is a more realistic test of this method's quality and provides a basis to address possible limitations.

The DNTMC methodology has been implemented in the NWChem computational chemistry package.[17] The Global Array (GA) Toolkit[18] has also been utilized to provide multilevel parallelization with respect to potential energy calculations and in running multiple simultaneous Markov chains. The potential energies of configurational states are determined by the Dang−Chang polarizable potential for water,[5] also available in the NWChem package. A total of ten simultaneous Markov chains are utilized in each calculation in which their average is presented as the probability distribution. Each Markov chain is started at a unique, randomly determined configuration, which along with the other Markov chains is evenly distributed along the radial coordinate. TeS is performed on each Markov chain independently and the resulting distributions are averaged as with the conventional simulations.

There are $6i - 3$ total degrees of freedom in water clusters composed of i monomers. A number of degrees of freedom have been removed by the use of rigid monomers ($3i$) and a center of mass coordinate system (3). The probability distributions of configurations are given with respect to one of these degrees of freedom, r_{config}. This coordinate is the maximum distance from the origin (cluster center of mass) to the center of mass of a monomer. The incorporation of all other degrees of freedom describes a sphere, where r_{config} is the radius, which encloses the molecular cluster.

Trial moves in the MC simulation are attempted with an uncorrelated probability of $^1/_2$ which include translational and rotational moves. After each successful attempt, the potential is calculated and checked for acceptance. The last accepted configuration, after both attempted moves, is placed into the Markov chain. The maximum translational displacement is 0.04 Å and the maximum rotational displacement is 0.06 radians. For the purposes of the radial distributions a total of 100 equally sized bins along the coordinate are utilized. Configurations are assigned bins based on their radius calculated from the center of mass of the cluster.

DNTMC calculations are performed with water clusters of varying size. These clusters are relatively small ranging in size from dimers to pentamers. Calculations are performed with 4×10^6 configurations per Markov chain for a total of 4×10^7 configurations. Simulations at five different temperatures (243, 273, 303, 333, and 363 K) are performed without TeS (conventional simulations). TeS is then applied to the Markov chains obtained at 363 K to produce scaled results at 243, 273, 303, and 333 K. These scaled results are then compared to the conventional results at these temperatures. This comparison provides a basis to address the accuracy of the TeS methodology and emphasize its limitations.

Three distinct features are present in the probability distributions for the water dimer shown in Figure 2 at five different temperatures. A region of high probability around $r_{config} = 1.50$ Å corresponds to configurations where the water monomers are close together and interacting. A region of low probability follows between r_{config} values of 2.00 and 3.00 Å. This region corresponds to the kinetic bottleneck as the water monomers separate. The defining radius of the water dimer (r_{cut}) lies in this region. Finally, a region of monotonically increasing probability for r_{config} values greater than 4.00 Å corresponds to the entropic region where the interaction potential between monomers becomes flat and configurational space continues to increase. These three characteristic regions of the probability distribution are called the interaction, bottleneck, and entropic regions, respectively.

The relative importance of these regions are temperature dependent. The probability shifts from the interaction to the entropic region as temperature increases. This shift is indicative of the increasing importance of entropic contributions to the free energy. The bottleneck region also shows some temperature dependence in the location of r_{cut}. In general r_{cut} decreases as temperature increases, as shown for the water dimer in Table 2. However, the change in the probability is not as dramatic as in other regions of the probability distribution due to its low magnitude. Further complications arise from the flat nature of this region of the distribution and the fact that r_{cut} is defined as the minimum in this region. Also, r_{cut} can only be defined as precisely as the bins defined along the r_{config} coordinate. The r_{config} coordinate is plotted with values between 1.25 and 5.25 Å giving a bin width of 0.04 Å. Over the temperature range 243 to 303 K, r_{cut} only changes by 0.16 Å, which corresponds to four bins along r_{config}.

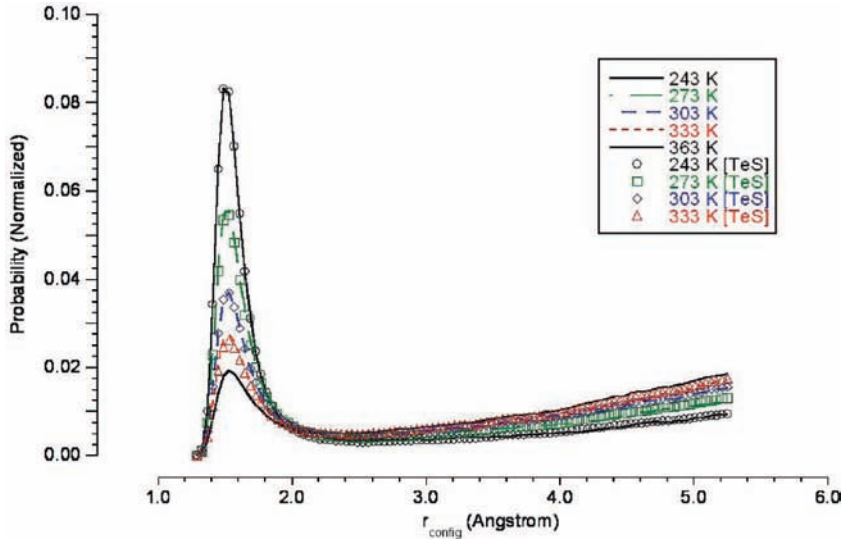

Figure 2. The radial distributions obtained from DNTMC calculations with the Dang−Chang potential on the water dimer at 5 different temperatures. r_{config} refers to the radius of a spherical volume centered at the center of mass. Values obtained via conventional MC methods are shown as lines whereas those obtained via TeS from a 363 K distribution are shown as open symbols.

TABLE 2: Comparison of Conventional and TeS DNTMC Calculations for the Water Dimer

temp (K)	r_{cut} (Å) conventional	r_{cut} (Å) TeS	$\alpha_i(T, r_{cut})$ (s^{-1}) conventional	$\alpha_i(T, r_{cut})$ (s^{-1}) TeS	R^2	max abs dev (prob)
243	2.53	2.53	1.75×10^{11}	1.63×10^{11}	1.000	5.52×10^{-4}
273	2.45	2.53	3.16×10^{11}	2.93×10^{11}	0.998	1.31×10^{-3}
303	2.57	2.49	4.66×10^{11}	4.55×10^{11}	0.998	5.47×10^{-4}
333	2.37	2.49	6.41×10^{11}	6.30×10^{11}	0.991	1.56×10^{-3}
363	2.37		8.56×10^{11}			

TABLE 3: Comparison of Conventional and TeS DNTMC Calculations for the Water Trimer

temp (K)	r_{cut} (Å) conventional	r_{cut} (Å) TeS	$\alpha_i(T, r_{cut})$ (s^{-1}) conventional	$\alpha_i(T, r_{cut})$ (s^{-1}) TeS	R^2	max abs dev (prob)
243	4.13	4.22	4.91×10^{10}	5.19×10^{10}	0.993	4.31×10^{-3}
273	4.04	4.04	1.57×10^{11}	1.60×10^{11}	0.971	4.89×10^{-3}
303	3.77	3.77	3.30×10^{11}	3.48×10^{11}	0.974	1.89×10^{-3}
333	3.68	3.68	6.08×10^{11}	5.90×10^{11}	0.994	1.06×10^{-3}
363	3.64		8.58×10^{11}			

TeS distributions obtained for four temperatures (243, 273, 303, and 333 K) reproduce the temperature dependence of the water dimer probability distributions, as shown in Figure 2. Since the maximum temperature change obtained from the distribution at 363 K with eq 5 is 255.6 K, TeS can be performed on the 120 K temperature range. The maximum absolute deviations between the scaled and conventional simulations, shown in Table 2, are relatively small considering the value of the probability at any point in the distribution. These maximum deviations between distributions occur in the interaction or entropic regions. The smaller maximum absolute deviations at 243 and 303 K occur in the entropic region while the larger values at 273 and 333 K occur in the interaction region. Finally, the values of r_{cut} in the scaled distributions loosely correlate with the values in the conventional distributions, although they vary less with changes in temperature. While the local indicators of a good correlation between conventional and scaled distributions are apparent from a low maximum absolute deviation and similar locations for maxima and minima (r_{cut}), a more global measure of correlation is the squared correlation coefficient (R^2) which is greater than 0.99 for all temperatures of interest. These indicators firmly establish TeS as a viable method for producing distributions at multiple temperatures.

These probability distributions for the water dimer at various temperatures allow us, through application of Dynamical Nucleation Theory, to determine monomer evaporation rate constants. The values of these evaporation rate constants, $\alpha_i(T, r_{cut})$, between the conventional and TeS calculations are similarly close to one another as shown in Table 2. The relative maximum absolute deviation between rate constants occurs at 273 K and is 7.3%, which allows an overall R^2 value over all temperatures of 0.999. This reproducibility is also apparent in the activation energy obtained from these methods. A linear least-squares fit of an Arrhenius plot of the conventional and temperature-scaled rate constants gives activation energies of 2.29 and 2.41 kcal/mol, respectively.

Table 3 shows the results of temperature scaling on the distribution at 363 K to the set of four lower temperatures between 243 and 333 K for the water trimer. The range of the r_{config} coordinate used for this simulation is 1.25 to 5.75 Å giving a radial bin width of 0.045 Å. Once again, the maximum temperature change obtained from the distribution at 363 K with eq 5 is 126.9 K, which is larger than the attempted maximum temperature change of 120 K. The resulting TeS distributions are expected to be of high quality, even though the maximum temperature change is about half the value obtained for the water dimer. The maximum absolute deviations between the conventional and TeS distributions are larger than the water dimer case, especially for the lower temperatures of 243 and 273 K, although still small. The maximum absolute deviations for all temperatures lie in the interaction region and are within 5% to 15% of the corresponding conventional distribution's value. Although the comparison between conventional and TeS distributions shows additional variation, the associated R^2 values are greater than 0.97 for all four temperatures of interest. Also, the TeS values of r_{cut} correspond very closely with conventional calculations. Only at 243 K is there a significant deviation (0.09 Å) that corresponds to the width of two radial bins. The monomer evaporation rate constants are similarly consistent between conventional and TeS calculations. The maximum relative absolute deviation is only 5.6% of the conventional results, occurring at the lowest temperature investigated (243 K). Given the good agreement of $\alpha_i(T, r_{cut})$ between conventional and TeS calculations, it is not surprising that the activation energies

TABLE 4: Comparison of Conventional and TeS DNTMC Calculations

temp	r_{cut} (Å)		$\alpha_i(T, r_{cut})$ (s^{-1})			max abs
(K)	conventional	TeS	conventional	TeS	R^2	dev (prob)
			water tetramer			
243	5.16	5.02	1.37×10^{10}	7.17×10^{9}	0.996	8.01×10^{-3}
273	5.06	4.97	5.24×10^{10}	5.59×10^{10}	0.999	3.75×10^{-3}
303	5.11	4.92	1.92×10^{11}	2.20×10^{11}	0.992	2.04×10^{-3}
333	4.73	4.78	5.24×10^{11}	5.28×10^{11}	0.978	2.46×10^{-3}
363	4.35		1.03×10^{12}			
			water pentamer			
243	5.54	6.23	9.49×10^{9}	1.37×10^{10}	0.973	1.61×10^{-2}
273	6.07	6.23	4.53×10^{10}	5.73×10^{10}	0.986	7.95×10^{-3}
303	6.12	6.17	1.54×10^{11}	1.91×10^{11}	0.913	7.61×10^{-3}
333	5.07	5.49	5.04×10^{11}	4.92×10^{11}	0.952	2.26×10^{-3}
363	5.39		9.08×10^{11}			

derived from these rate constants similarly agree with values of 4.21 and 4.11 kcal/mol respectively for conventional and TeS results.

The results, shown in Table 4, for the water tetramer and pentamer are similar overall to those for the dimer and trimer. The range of the r_{config} coordinate used for these simulations is 1.50 to 6.25 Å for the tetramer and between 1.50 and 6.75 Å for the pentamer. The TeS distributions provide a good approximation to the conventionally obtained distributions with R^2 values greater than 0.9. The water tetramer, however, does have a maximum absolute deviation that is about a factor of 2 greater than that of the water trimer system. These maximum absolute deviations tend to increase as temperature decreases and are located in the interaction region of the distribution. The monomer evaporation rate constants, obtained from the TeS distributions, deviate no more than 15% from the conventional results. However, at 243 K the TeS result deviates by more than 45%. This large deviation causes the determined activation energy to change from 6.43 kcal/mol (for conventional calculations) to 7.26 kcal/mol. Although this change is less than 1 kcal/mol in magnitude, it is significantly more than the approximately 0.1 kcal/mol change in the water dimer and trimer cases. An explanation for the deviating results at 243 K between the conventional and TeS distributions can be found by examining the maximum temperature change determined by the distribution at 363 K by using eq 5. Unlike the dimer and trimer cases, the water tetramer is the first system studied in which this maximum temperature change, which is 66.69 K, is less than the maximum attempted temperature change of 120 K. This situation makes the quality of TeS distributions obtained for 243 and 273 K suspect. The use of one standard deviation unit in the formulation of the measure in eq 5 is fairly conservative. We find that using 1.5 standard deviation units makes this measure a little more predictive in terms of our comparisons between conventional and TeS distributions. By using 1.5 standard deviation units the maximum temperature change for the water tetramer is 100.0 K, making only the quality of results obtained at 243 K suspect.

The results for the water pentamer are similar to those for the water tetramer, also shown in Table 4. Once again the maximum temperature change obtained from the distribution at 363 K with eq 5 is less than 120 K. By using 1.5 standard deviation units in this expression the maximum temperature change is 75.57 deg, which makes the quality of results obtained at 273 and 243 K suspect. The maximum absolute deviation between conventional and TeS distributions is about a factor of 2 larger than those present in the water tetramer case. These deviations also tend to increase as temperature decreases. The

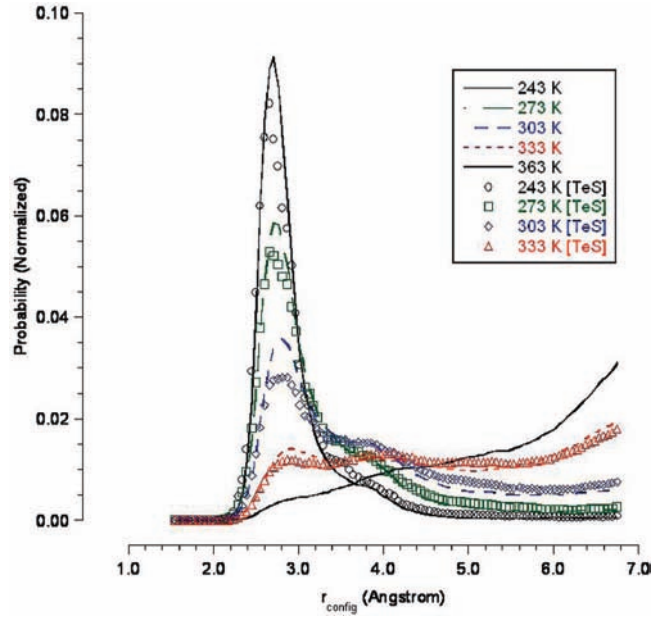

Figure 3. The radial distributions obtained from DNTMC calculations using the Dang−Chang potential on the water pentamer at 5 different temperatures. r_{config} refers to the radius of a spherical volume centered at the center of mass. Values obtained via conventional MC methods are shown as lines whereas those obtained via TeS from a 363 K distribution are shown as open symbols. Note the deviations between the TeS distributions and their corresponding conventional distributions. These deviations are caused by entropic effects which diminish the sampling in the interaction region.

values of r_{cut} also suffer from increased deviation between the conventional and TeS distributions. At 243 K, the lowest temperature, r_{cut} differs by 0.69 Å. These deviations between the conventional and TeS distributions also manifest themselves in the monomer evaporation rate constants, shown in Table 4. At 243 K, the TeS result is 44.5% larger than the corresponding conventional result. This deviation, similar to the probability distribution shown in Figure 3, increases as temperature decreases from 363 K. However, the activation energies obtained from the conventional and TeS evaporation rate constants are similar with values of 6.80 and 6.22 kcal/mol, respectively. This deviation (0.58 kcal/mol) although smaller than in the tetramer case is still significantly more than either the dimer or trimer cases.

The diminished effectiveness of the TeS method in providing accurate probability distributions at increasing lower temperatures for the tetramer and pentamer systems is attributed to the increasing influence of entropy. Figures 2 and 3 for the water dimer and pentamer show an increasing importance in the entropic region as temperature increases. At 363 K the dominance of the interaction region is largely diminished in the probability distribution. Comparing the probability distribution at 363 K for the dimer and pentamer systems, the interaction region is diminished more for the pentamer. A result of this interaction region depletion can be seen in Figure 3 where the TeS distributions deviate from the conventional distributions.

The correlation between entropic changes and the chosen coordinate (r_{config}) can be seen by examining the extent of configurational space that is contained within this spherical volume. The extent of configurational space increases by 6 degrees of freedom for each additional monomer in the cluster. These degrees of freedom correspond to 3 translational and 3 rotational degrees of freedom. The rotational degrees of freedom can be equated to an equivalent volume expressed as r^{3i}, where

r refers to the monomer radius, which is not dependent on r_{config}. The translational degrees of freedom can be equated to an equivalent spherical volume (based on r_{config}) as $V_{eq} \propto r_{config}^{3i-3}$. The extent of configurational space increases as increasing powers (as monomers are added) of r_{config} along this coordinate. For large values of r_{config} where the interaction between monomers is least, there is an increased likelihood of entropic contributions.

The effect of entropic contributions on the effectiveness of the TeS method is a very system dependent question. For the 1-D analytical potential, entropic considerations did not affect the resulting distributions. However, for the water molecular clusters entropy plays an ever increasing role as the size (number of monomers) of these clusters increases. This system dependence can also be seen by looking at the maximum temperature changes determined by eq 5. This temperature change is very large for the 1-D analytical potential. For the water cluster systems, this temperature change decreases rapidly as monomers are added to the system. Therefore, the quality of TeS distributions diminishes for large temperature changes. Systems differing from the ones presented in this work will undoubtedly have different dependencies concerning entropic contributions. A short list of important factors are the topography of the potential energy surface, choice of coordinate for the analysis of statistical properties, and system model. The straightforward analysis of entropic effects in the water molecular clusters in this work is aided by the combination of all three of these factors. Therefore, the advantageous result that links the r_{config} coordinate with entropic contributions should be viewed as specific to these kinds of systems.

6. Statistical Properties

So far emphasis has focused on probability distributions based on monitoring a degree of freedom. Since the TeS method scales a Markov chain by the individual weighting of its members, it is very general and does not depend on the coordinate chosen to construct probability distributions. Therefore unlike methods which utilize corrections along a particular coordinate,[7,19] TeS Markov chains can be utilized to determine various statistical quantities. To illustrate this capability, we present conventional and TeS distributions at 243 K for the water trimer. Two probability distributions are investigated. The first is the oxygen−oxygen (O−O) distance, shown in Figure 4. The second is the potential energy distribution, shown in Figure 5. Table 5 shows numerical characteristics of these probability distributions for the dimer and trimer systems at 243 K.

The probability distributions presented in this section illustrate the determination of statistical properties of molecular clusters. As such, DNT[15,16] defines the molecular cluster as consisting of all configurations which have $r_{config} \leq r_{cut}$. To keep our descriptions consistent, only configurations fitting this definition have been incorporated in the probability distributions. Similar to our previous utilization of the TeS method, TeS distributions are obtained from Markov chains obtained at 363 K.

Figure 4 shows the O−O distance distribution for the water trimer at 243 and 363 K. Each of the three corresponding distances have been included in these distributions. At 363 K, the distribution is more spread out than at 243 K. However, at both temperatures there is a significant peak in probability around 3.0 Å. This corresponds to an O−O distance consistent with hydrogen bonding. The TeS distribution at 243 K very closely resembles the conventional distribution with a difference in the thermally averaged O−O distance (⟨O−O⟩) of 0.05 Å, as shown in Table 5.

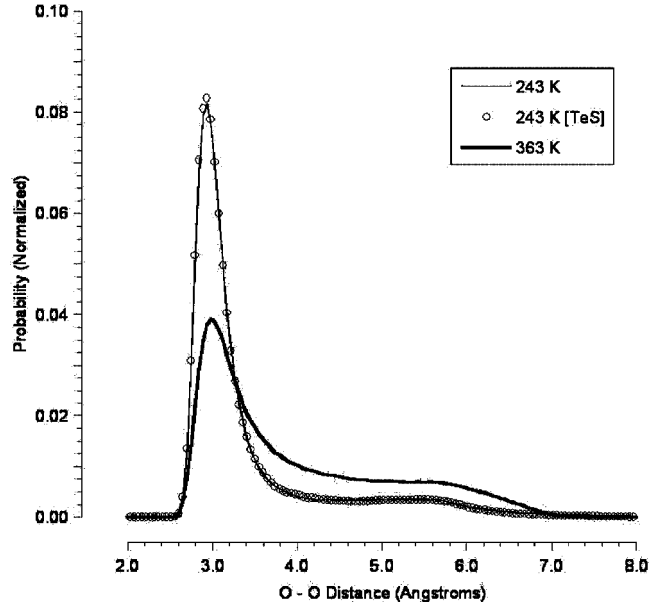

Figure 4. The oxygen−oxygen (O−O) distance distribution for the water trimer. Conventional MC distributions at 243 and 363 K are given as lines along with a TeS distribution at 243 K (obtained from 363 K) shown as open symbols.

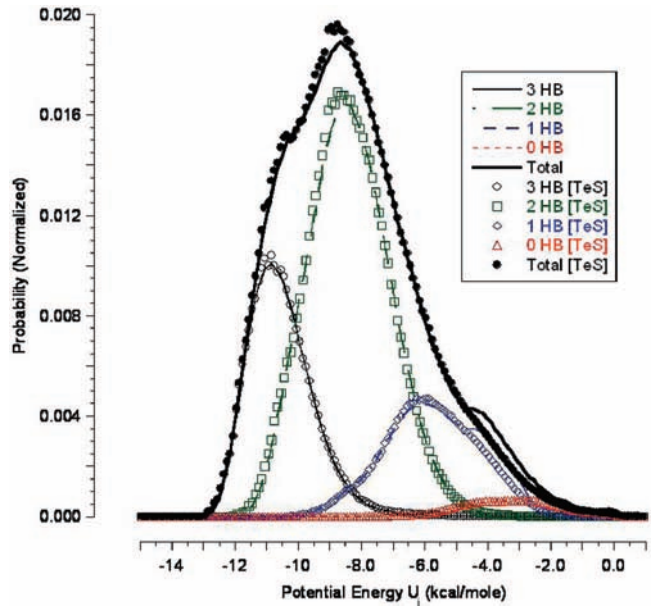

Figure 5. The potential energy distributions for the water trimer at 243 K. Both conventional (lines) and TeS distributions (open symbols) are shown. The total distribution is given along with its decomposition into component distributions having between 0 and 3 hydrogen bonds (HB). TeS was performed on the MC distribution obtained at 363 K.

Figure 5 shows the potential energy distributions for the water trimer at 243 K. This distribution has been further decomposed into four components. Each component corresponds only to those configurations which approximately contain a certain number of hydrogen bonds (0−3). The configurations have been grouped into these categories by graphical inspection in which a hydrogen bond is defined by a characteristic hydrogen−oxygen distance between 1.5 and 2.5 Å and an oxygen−hydrogen−oxygen angle ≥120°.[20] The TeS distributions closely match the conventional distributions. Further analysis of these distributions is presented in Table 5 for the dimer and trimer systems. Two properties have been determined from these distributions, the

TABLE 5: Comparison of Conventional and TeS Distributions at 243 K

	⟨O−O⟩ (Å)	
	conventional	TeS
dimer	3.27	3.23
trimer	3.46	3.41

	dimer			
	conventional		TeS	
	1 HB	0 HB	1 HB	0 HB
$\langle U_i \rangle$ (kcal/mol)	−3.33	−1.44	−3.33	−1.51
occupation (%)	68.97	31.03	71.04	28.96

	trimer							
	conventional				TeS			
	3 HB	2 HB	1 HB	0 HB	3 HB	2 HB	1 HB	0 HB
$\langle U_i \rangle$ (kcal/mol)	−10.52	−8.37	−5.63	−2.96	−10.52	−8.39	−5.78	−3.28
occupation (%)	24.38	54.07	18.58	2.97	24.87	54.96	17.60	2.56

thermal average of the potential energy ($\langle U_i \rangle$) and the percent occupation of each component with respect to the total distribution. These properties closely correspond between the conventional and TeS distributions. The thermal average potential energy varies by much less than a kilocalorie per mole and the percent occupation similarly agrees within about a percent.

7. Conclusion

These results rigorously establish TeS as a viable method capable of producing statistics at multiple temperatures for a wide range of properties from a single Markov chain. Unlike Weighted Histogram analysis, distributions other than energy may be gathered from the TeS Markov chain for analysis. From our studies of a 1-D model potential, this method has the potential for use as a way to circumvent quasiergodic behavior at low temperatures. MC simulations can be performed at a high temperature in which quasiergodicity is not an issue. Then TeS can be applied to produce statistics at lower temperatures where quasiergodicity is an issue with conventional MC simulations. The maximum temperature change obtained from eq 5 can also be reliably used as a measure of the quality of TeS results prior to scaling and without knowledge of the exact distributions. This measure inherently defines the limitations of the TeS method. Scaling can only be performed within the confines of the original MC simulation. Namely the average potential energy cannot shift beyond the range sampled by the original distribution and large temperature changes have an increased possibility of shifting this property beyond this limit.

A large number of calculations proportional to the number of temperatures of interest can be avoided by TeS Markov chains obtained at a high temperature to produce statistics at lower temperatures. However, a limitation is present in the form of entropic contributions which cause inadequate sampling of low potential energy configurations. In our water cluster systems, an advantageous correlation between the r_{config} coordinate and increasing configurational space makes analysis of the effects of increasing entropic contributions relatively straightforward. At sufficiently high temperatures, entropy becomes increasingly important (even more so than potential energy). This is evident by a shift in the probability to higher values of r_{config} as temperature increases. Also this effect occurs more rapidly for larger clusters (those with more monomers). At some high temperature, as a result of this probability shift, there is a detachment of the distribution from lower values of r_{config} which contain configurations that have lower potential energies—meaning that entropic effects have become so important that the high-temperature Markov chain predominately samples the higher potential energy configurations in lieu of the lower potential energy configurations. This entropic influence is also present in the maximum temperature change determined from eq 5 through its inverse dependence on the heat capacity at constant volume. As entropy becomes more important in a system, the heat capacity generally increases, which describes the situation where more energy is required to change the temperature of the system by a specified amount. This decreases the maximum temperature change for which TeS is appropriate. However, this situation does not represent a deficiency in sampling. For the distribution to accurately describe the free energy of the system, entropy must become increasingly important as temperature increases.

In future work, larger sized clusters will be examined to determine the extent to which TeS will provide useful data. In particular, extrapolations to larger systems on the order of 10^3 to 10^5 particle systems will be performed where the usual temperature spacing for the Parallel Tempering method is approximately 3−5 K. In addition, it should be possible to combine TeS and Parallel Tempering to improve the overall efficient computation of properties at many temperatures.

Acknowledgment. T.L.W. and L.D.C. gratefully acknowledge Iowa State University and Ames Laboratory for funding and computational resources. This work was performed in part using the Molecular Science Computing Facility (MSCF) in the William R. Wiley Environmental Molecular Sciences Laboratory, a DOE national scientific user facility located at the Pacific Northwest National Laboratory (PNNL). PNNL is operated by Battelle for the U.S. Department of Energy.

References and Notes

(1) Metropolis, N.; Ulam, S. *J. Am. Stat. Assoc.* **1949**, *44*, 335.
(2) Metropolis, N.; Rosenbluth, A. W.; Rosenbluth, M. N.; Teller, A. H.; Teller, E. *J. Chem. Phys.* **1953**, *21*, 1087.
(3) (a) Day, P. N.; Jensen, J. H.; Gordon, M. S.; Webb, S. P.; Stevens, W. J.; Krauss, M.; Garmer, D.; Basch, H.; Cohen, D. *J. Chem. Phys.* **1996**, *105*, 1968. (b) Chen, W.; Gordon, M. S. *J. Chem. Phys.* **1996**, *105*, 11081. (c) Merrill, G. N.; Gordon, M. S. *J. Phys. Chem. A* **1998**, *102*, 2650. (d) Day, P. N.; Pachter, R.; Gordon, M. S.; Merrill, G. N. *J. Chem. Phys.* **2000**, *112*, 2063. (e) Gordon, M. S.; Freitag, M. A.; Bandyopadhyay, P.; Jensen, J. H.; Kairys, V.; Stevens, W. J. *J. Phys. Chem. A* **2001**, *105*, 293.
(4) Jorgensen, W. L.; Chandrasekhar, J.; Madura, J. D.; Impey, R. W.; Klein, M. L. *J. Chem. Phys.* **1983**, *79*, 926.
(5) Dang, L. X.; Chang, T.-M. *J. Chem. Phys.* **1997**, *106*, 8149.
(6) Crosby, L. D.; Kathmann, S. M.; Windus, T. L. *J. Comput. Chem.* Accepted for publication.
(7) Ferrenberg, A. M.; Swendsen, R. H. *Phys. Rev. Lett.* **1988**, *61*, 2635.
(8) Ferrenberg, A. M.; Swendsen, R. H. *Phys. Rev. Lett.* **1989**, *63*, 1195.
(9) Frantz, D. D.; Freeman, D. L.; Doll, J. D. *J. Chem. Phys.* **1990**, *93*, 2769.
(10) Zhou, R.; Berne, B. J. *J. Chem. Phys.* **1997**, *107*, 9185.
(11) Geyer, C. J.; Thompson, E. A. *J. Am. Stat. Assoc.* **1995**, *90*, 909.
(12) Swendsen, R. H.; Wang, J. S. *Phys. Rev. Lett.* **1986**, *57*, 2607.
(13) Brown, S.; Head-Gordon, T. *J. Comput. Chem.* **2002**, *24*, 68.
(14) Kathmann, S. M.; Palmer, B. J.; Schenter, G. K.; Garrett, B. C. *J. Chem. Phys.* **2008**, *128*, 064306.
(15) Schenter, G. K.; Kathmann, S. M.; Garrett, B. C. *J. Chem. Phys.* **1999**, *110*, 7951.
(16) Schenter, G. K.; Kathmann, S. M.; Garrett, B. C. *Phys. Rev. Lett.* **1999**, *82*, 3484.
(17) (a) Bylaska, E. J.; de Jong, W. A.; Kowalski, K.; Straatsma, T. P.; Valiev, M.; Wang, D.; Aprà, E.; Windus, T. L.; Hirata, S.; Hackler, M. T.; Zhao, Y.; Fan, P.-D.; Harrison, R. J.; Dupuis, M.; Smith, D. M. A.; Nieplocha, J.; Tipparaju, V.; Krishnan, M.; Auer, A. A.; Nooijen, M.;

Brown, E.; Cisneros, G.; Fann, G. I.; Früchtl, H.; Garza, J.; Hirao, K.; Kendall, R.; Nichols, J. A.; Tsemekhman, K.; Wolinski, K.; Anchell, J.; Bernholdt, D.; Borowski, P.; Clark, T.; Clerc, D.; Dachsel, H.; Deegan, M.; Dyall, K.; Elwood, D.; Glendening, E.; Gutowski, M.; Hess, A.; Jaffe, J.; Johnson, B.; Ju, J.; Kobayashi, R.; Kutteh, R; Lin, Z.; Littlefield, R.; Long, X.; Meng, B.; Nakajima, T.; Niu, S.; Pollack, L.; Rosing, M.; Sandrone, G.; Stave, M.; Taylor, H.; Thomas, G.; van Lenthe, J.; Wong, A.; Zhang, Z. *NWChem*, A Computational Chemistry Package for Parallel Computers, Version 5.0; Pacific Northwest National Laboratory, Richland, WA, 2006. (b) Kendall, R. A.; Aprà, E.; Bernholdt, D. E.; Bylaska, E. J.; Dupuis, M.; Fann, G. I.; Harrison, R. J.; Ju, J.; Nichols, J. A.; Nieplocha, J.; Straatsma, T. P.; Windus, T. L.; Wong, A. T. *Comput. Phys. Commun.* **2000**, *128*, 260–283.

(18) Nieplocha, J.; Palmer, B.; Tipparaju, V.; Krishnan, M.; Trease, H.; Apra, E. *Int. J. High Perf. Comput. Appl.* **2006**, *20*, 203.

(19) (a) Ming, Y.; Lai, G.; Tong, C.; Wood, R. H.; Doren, D. J. *J. Chem. Phys.* **2004**, *121*, 773. (b) Liu, J.; Yang, L.; Doren, D. J. *Chem. Phys. Lett.* **2006**, *417*, 63. (c) Liu, J.; Yang, L.; Doren, D. *J. Chem. Phys.* **2006**, *323*, 579.

(20) Crosby, L. D.; Windus, T. L., future work to be published. The parameters used to distinguish hydrogen bonding interactions in the structure of configurations were determined through MC simulations of the water trimer. A future publication will provide more detail in the results of these simulations.

JP805688J